Materials Research Proceedings 41 (2024) 2796-2804 https://doi.org/10.21741/9781644903131-306

Influence of surface treatments on the fatigue strength of cross bores in shafts from EN-GJS700-2

UHLMANN Lars[1,a*], DADGAR Mohammad[1,b], MÜLLER Martina[1,c], HERRIG Tim[1,d] and BERGS Thomas[1,2,e]

[1] Manufacturing Technology Institute MTI of RWTH Aachen University, Campus-Boulevard 30, 52074 Aachen, Germany

[2] Fraunhofer Institute for Production Technology IPT, Steinbachstraße 17, 52074 Aachen, Germany

[a]l.uhlmann@mti.rwth-aachen.de, [b]m.dadgar@mti.rwth-aachen.de, [c]m.mueller@mti.rwth-aachen.de, [d]t.herrig@mti.rwth-aachen.de, [e]t.bergs@mti.rwth-aachen.de

Keywords: Deep Rolling, Residual Stresses, Shot Peening, Induction Hardening

Abstract. The European Union's Federal Climate Protection Act mandates a 55 % reduction in greenhouse gas emissions from 1990 levels by 2030, aiming for climate neutrality by 2050. Achieving these goals requires emission cuts across sectors, including energy, industry, and transportation. Lightweight design in transportation, achieved through alternative materials, geometry optimization, or enhanced fatigue strength, is vital. Highly stressed components like shafts are prone to failure due to notch locations which reduces the fatigue strength significantly. Inducing compressive residual stresses through methods like deep rolling and shot peening may improve the fatigue strength by reducing critical tensile load stresses. This study compares the fatigue strength of shaft cross bores treated with induction hardening, deep rolling, shot peening, and the combination of induction hardening and deep rolling. The research aims to establish a cause-effect relationship between surface layer properties and fatigue strength, considering the redistribution of residual stresses during testing.

Introduction

The Federal Climate Protection Act was enacted in the European Union to mitigate anthropogenic climate change. According to the act, greenhouse gas emissions must be reduced by 55 % from 1990 levels by 2030 and become climate neutral by 2050 [1]. To achieve these ambitious climate targets, it is necessary to reduce greenhouse gas emissions in all relevant areas, including the energy, industry, and transport sector. In the transport sector, lightweight design is often pursued to reduce component weight, leading to lower material usage and energy requirements during operation. This can be achieved through the use of alternative materials [2], geometry optimization [3],or increased fatigue strength of existing components [4]. The latter term is used specifically for components that are subjected to high levels of stress. One example of highly stressed components in the transport sector are shafts. The fatigue strength of shafts is limited by notch locations, such as shaft heels or cross bores, as these usually represent the starting point for structural failure, such as crack initiation and crack growth [5]. To increase the fatigue strength of shafts, the surface layer is inductively hardened [6] or compressive residual stresses are induced into the surface layer [7]. The depth effect of inductive hardening is limited, which limits the influence on cross bores in particular. The compressive residual stresses counteract the critical tensile load stresses, which increases the fatigue strength [8]. Typical processes for inducing compressive residual stresses are deep rolling and shot peening. Both processes are mechanical surface treatments in which local plastic deformation induces compressive residual stresses. The compressive residual stresses are typically direction-dependent after deep rolling [9] and direction-independent after shot peening

[10]. During deep rolling, the compressive residual stresses are typically lower in the feed direction than perpendicular to it. In both processes, the hardness and roughness are modified in addition to the residual stresses. The roughness after deep rolling is typically lower than after shot peening. This is due to the stochastic characteristics of shot peening compared to the deterministic deep rolling. The influence of shot peening of cross bores in shafts from EN-GJS-700-2 and 34CrNiMo6 +QT on the fatigue strength was investigated by Reissner et al [11]. In the work it was shown, that shot peening influences the slope of the S-N curve due to a redistribution of residual stresses. Transferring the results to deep rolled cross bores is not necessarily possible because the residual stress distribution and roughness characteristics are different from those after shot peening. Accordingly, the influence of the surface layer properties of especially deep rolled but also shot peened cross bores on the fatigue strength is insufficiently investigated. The aim of the work is therefore to determine the cause-effect relationships between the surface layer properties set by shot peening and deep rolling on the fatigue strength of shafts with cross bores. For this purpose, experimental fatigue strength tests were carried out on analogous specimens made of EN-GJS-700-2 with untreated, induction hardened, deep rolled, shot peened and induction hardened and subsequently deep rolled cross bores. In addition to the fatigue strength tests, the surface layer properties were characterized on the basis of residual stresses, roughness, fracture pattern, microstructure and hardness. In addition, the redistribution of the residual stresses was considered for the interpretation of the fatigue strength results (compare [11] for shot peening and [12] for deep rolling).

Materials and Methods

The fatigue strength of shafts with cross bores was investigated using analogy specimen to reduce the complexity of the setup. The geometry of the specimen is shown in Figure 1 (a). The specimen from EN-GJS-700-2 feature a cross bore with a diameter of d_B = 5 mm in the center. The initial cross bore was manufactured by drilling and then reaming. A high-speed steel drill with a diameter of d_{Drill} = 4.8 mm was used for drilling at a feed rate of F_{Drill} = 100 mm·min^{-1} and a rotational speed of n_{Drill} = 1600 min^{-1}. A reamer made of high-speed steel with a diameter of 5H7 was used for reaming and operated at a feed rate of F_{Ream} = 100 mm·min^{-1} and a rotational speed of n_{Ream} = 630 min^{-1}.

The cross bore was subsequently post-processed. A total of seven different variants were considered as part of the investigations. Two reference variants based on industrial applications were used. Furthermore, two shot-peened and two deep rolled variants were considered, as well as one variant that was first induction hardened and then deep rolled.

Referent variants. The reference variants considered were an untreated (REF) and an induction hardened variant (IND). The REF variant was not further post-processed. For the IND variant the shaft surface of the specimen was induction hardened to a hardness of H_{IND} = 52-53 HRC with a hardness depth of t_{IND} = 3 mm. The induction hardened area is shown in Figure 1 (a).

Shot peened variants. Two variants with different process parameter setups SP1 and SP2 were considered. The shot peening parameters as well as the fatigue results are described in the work of Reissner et al. and were used as comparison within this work especially by means of the different residual stress distribution after shot peening and deep rolling [11].

Deep rolled variants. Deep rolling was conducted by Ecoroll AG using a hydrostatic deep rolling tool with a tool diameter of d_W = 2.38 mm. Two different deep rolling setups (DR1 and DR2) were considered. For DR1 a deep rolling pressure of p_W = 400 bar and a feed of f_W = 0.062 mm and for DR2 a deep rolling pressure of p_W = 250 bar and a feed of f_W = 0.054 mm were applied.

Induction hardened and deep rolled variant. The induction hardened and then deep rolled variant (IND + DR1) was first induction-hardened according to the IND variant and then deep-rolled according to DR1.

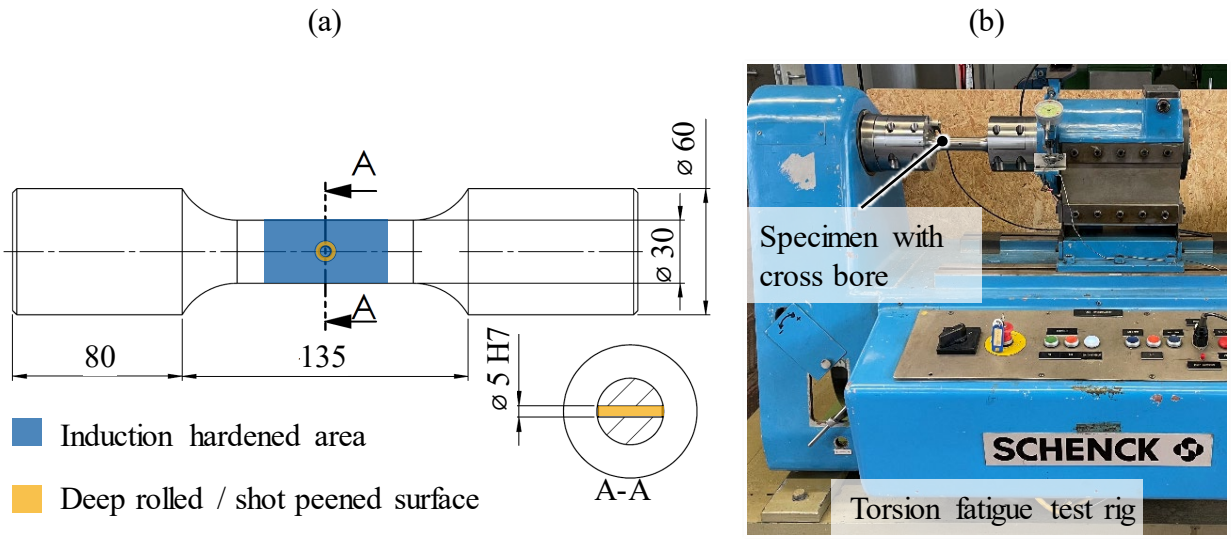

Figure 1: Geometry of specimen used (a) and experimental setup for torsion fatigue tests

Torsional fatigue strength tests. The torsional fatigue strength of the specimen was tested on a FLATO of Schenk at the Institute for Materials Applications in Mechanical Engineering IWM of RWTH Aachen University (see Figure 1 (b)). The tests were carried out in the finite life fatigue area with a torque ratio of R_T = -1. The test frequency was f = 25 Hz and the maximum number of load cycles was $N_m = 5 \cdot 10^6$.

Analysis of surface layer properties. To understand the cause effect relationship between the surface treatments and the resulting fatigue strength the roughness, the microhardness, the fracture pattern and the residual stresses within the cross bore were considered. The roughness of the cross bore surface was determined using a Hommel-Etamic nanoscan 855 tactile contour and roughness measuring device from JENOPTIK Industrial Metrology Germany GmbH. Measurements were taken in three areas of the cross bore, namely in the area of the chamfer on both sides and in the center of the cross bore. Three measurements were carried out in each area for statistical assurance. The roughness measurements were evaluated in accordance with DIN EN ISO 4288. The evaluation was based on the mean roughness depth *Rz* and the arithmetic mean roughness *Ra*. The microhardness test was carried out in accordance with DIN EN ISO 14577-1 on a Fischerscope HM2000 from Helmut Fischer and converted into Vickers hardness. To determine the microhardness in the cross bore, metallographic sections of the analogy specimens in the area of the cross bore were used. The test force was F_{HM} = 490 mN, which was applied over a period of t = 20 s. The holding time during the hardness test was T_{hold} = 10 s. The subsequent reduction in force also took place over a period of t = 20 s.The fracture patterns were analyzed using reflected light microscope images and scanning electron microscope (SEM) images. The residual stresses were recorded using X-ray diffraction (XRD) measurements with an Xstress G2R with a Mythen detector from Stresstech GmbH. The combination of XRD measurement, electrochemical etching with a Polimat from Buehler and depth measurements using a dial gauge with an alignment using a MarSurf GD 120 tactile feed device from Mahr was used to determine residual stress depth curves.

In addition to the residual stress measurements of the specimen as manufactured, the redistribution of the residual stresses due to cyclic loading was taken into account both experimentally and numerically (see [12]). In addition to the residual stresses, the load stress distribution due to the torsional load was taken into account using finite element (FE) simulations. The simulation model presented in Uhlmann et al. was used, although no residual stresses were considered, and the calculation was simplified using a purely elastic material model [12].

Results and Discussion

Observations. In Figure 2 the results of the torsional fatigue strength by means of S-N curves are shown. The following observations were made on terms of the results:

- Comparing the references (REF and IND), the induction hardened specimen has a higher fatigue strength, while the slope of the S-N curve is similar.
- Comparing the deep rolled (DR1, DR2 and IND + DR1) and the shot peened (SP1 and SP2) variants to the references (REF and IND) a different slope is observed, resulting in a higher fatigue strength for lower load amplitudes.
- The fatigue strength of the shot peened (SP1 and SP2) variants for a lower load amplitude is higher than for the deep rolled (DR1 and DR2) variants.
- The fatigue strength for the induction hardened and deep rolled (IND + DR1) is increased and the slope is improved compared to REF.
- The breakage of some IND + DR1 specimen is shifted out of the cross bore.

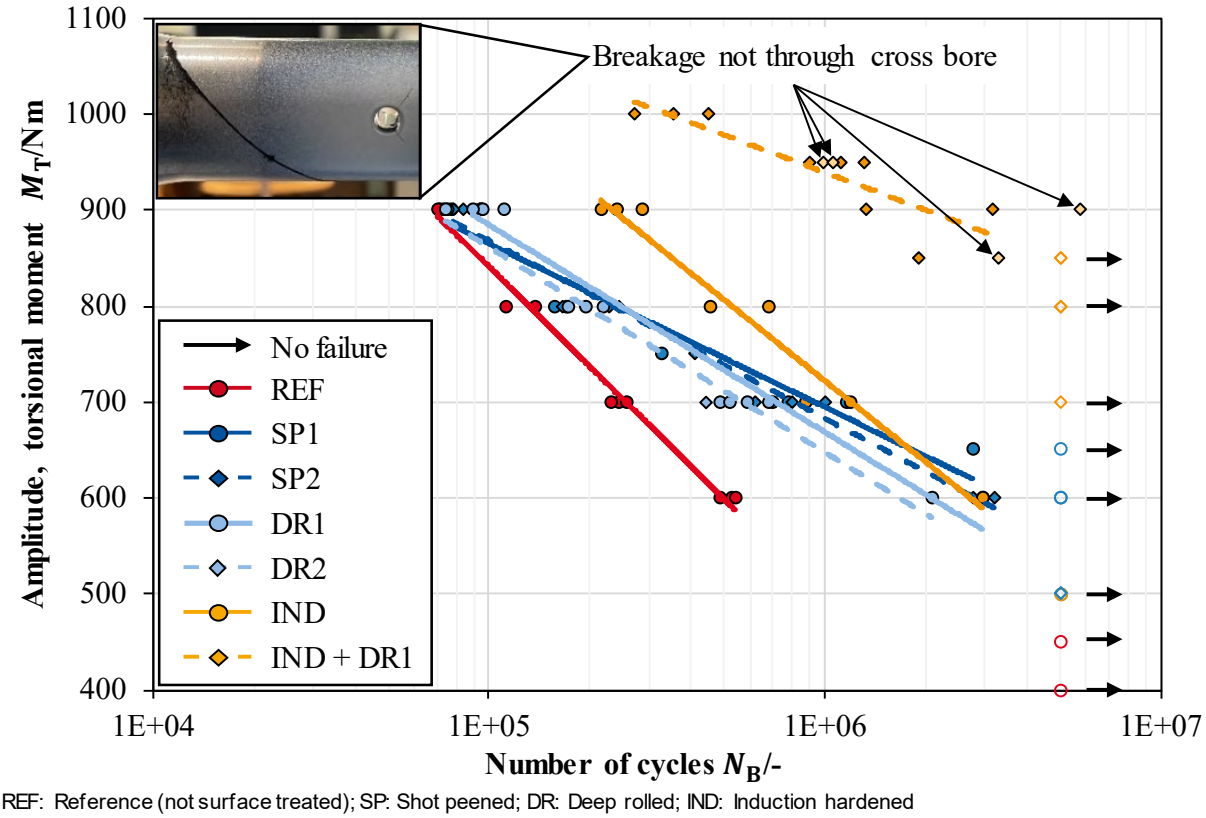

Figure 2: Fatigue strength results

Explanation approach. In the following, only the results of the surface layer properties were presented, based on which the explanatory approaches were derived. It is to say, that the explanatory approaches are not invalidated by the additional results not shown.

The increase of fatigue strength of the IND specimen compared to the REF specimen may be explained on the basis of the crack initiation. In Figure 3 (a) the fracture pattern of the REF and the IND specimen are juxtaposed. The crack initiation location of the hardened specimen is shifted to the inside of the bore, where the load stresses are lower than at the crack initiation location of the REF specimen resulting in the higher fatigue strength. In Figure 3 (b) the relative decrease of the load stresses is plotted over the distance to the chamfer into the bore for a shaft diameter of d_s = 30 mm to reinforce the explanation approach. While the load stresses at the crack initiation of

the REF specimen were at the maximum, the load stresses at the crack initiation of the IND specimen were about 30 % reduced.

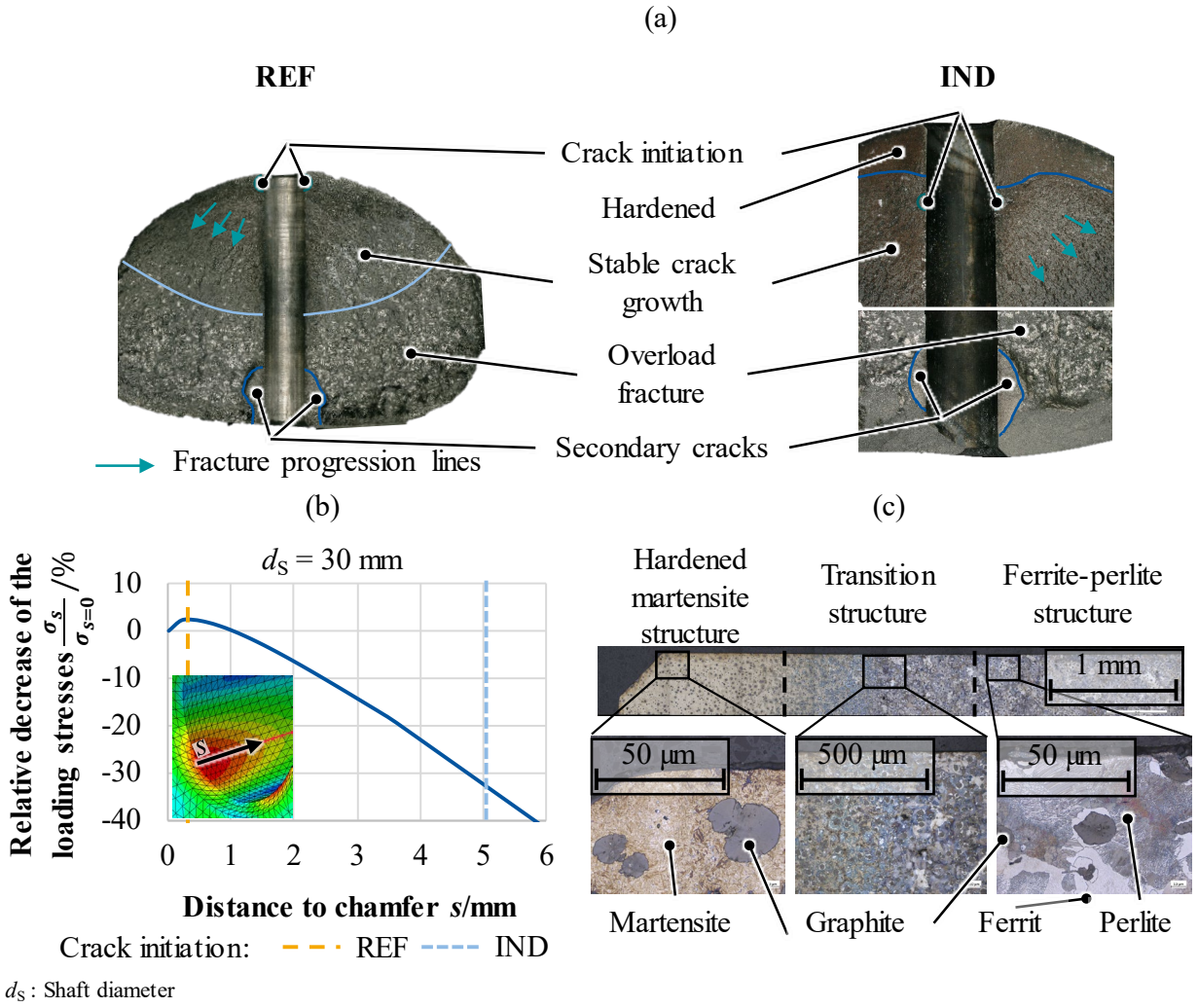

d_S : Shaft diameter

Figure 3: Comparison of fracture pattern of REF and IND specimen (a), numerically obtained load stresses depending on the distance to chamfer (b) and microstructure of IND specimen (c)

The shift of the crack initiation location of the INT specimen into the cross bore is explained due to the hardened surface layer as a result of martensite transformation. In its initial state, EN-GJS-700-2 has a ferritic-pearlitic microstructure with spheroidal graphite inclusions. Due to hardening, the surface layer is transformed into martensite (see Figure 3 (c)). The higher hardness also results in reduced crack growth, which can be seen in the fracture patterns from the lower roughness in the hardened area compared to the area of the original material.

The residual stresses and especially the redistribution of the residual stresses in the area of crack initiation offer a possible explanation for the different slopes of the S-N curve comparing the deep rolled or shot peened variants with the reference variants. In Figure 4 (a) the tangential stress graphs for DR1 and SP1 after loading are compared to the residual stresses before loading. A qualitative comparison of the graphs for the different loads show that the redistribution of residual stresses is more pronounced at higher loads. Therefore, the influence of the residual stresses induced by deep rolling and shot peening on the fatigue strength is less pronounced. Accordingly, the slope of the S-N curve is improved compared to the REF variant.

(a) (b)

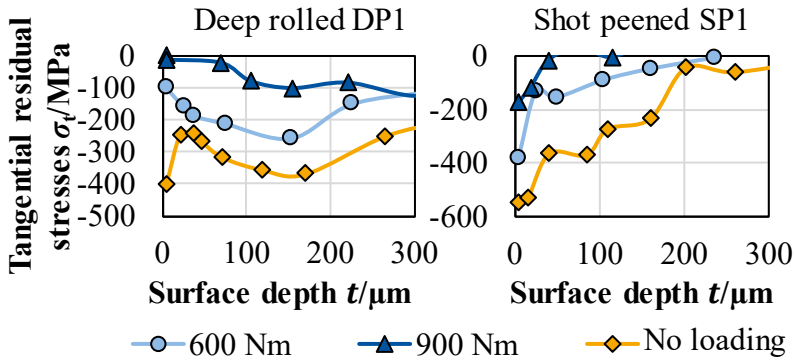

Variant	Tangential residual stresses σ_t in MPa	Axial residual stresses σ_a in MPa
SP1	-544	-544
DR1	-401	-899
DR2	-354	-827

Figure 4: Redistributed residual stresses (a) and residual stresses at the cross bore surface after deep rolling and shot peening (b)

The fatigue strength of the shot peened (SP1 and SP2) variants is higher than that of the deep rolled (DR1 and DR2) variants under lower loadings due to the induced residual stresses and load stresses. Torsional loading results in tangential load stresses in the bore, and the tangential residual stresses counter the load stresses. Figure 4 (b) shows the tangential and axial residual stresses at the surface of the bore for the shot peened variant SP1 and the deep rolled variants DR1 and DR2. The residual stresses in both directions are homogeneous after shot peening. However, after deep rolling, the tangential residual stresses are lower and the axial residual stresses are higher than after shot peening, resulting in lower fatigue strength. For this case, the results indicate that residual stresses have a more significant impact on fatigue strength than roughness. This is because the deep rolled variants have a lower roughness than the shot peened variants which suggests increased fatigue strength.

The increased fatigue strength and improved slope of the S-N curve of the IND + DR1 variant can be explained by the compressive residual stresses described above as well as the shift of the crack initiation location. Induction hardening shifts the crack initiation location into the bore, resulting in reduced load stresses at the crack initiation location (compare Figure 3). Deep rolling induces compressive residual stresses in the surface area of the specimen (compare Figure 4). This is particularly important because, due to the larger volume of martensite in the hardened region compared to the ferrite-pearlite structure, it can be assumed that compressive residual stresses are present in the hardened region and, prior to deep rolling, tensile residual stresses are present in the transition area, where the crack initiation is located. The compressive residual stresses counteract the critical tensile load stresses increasing the fatigue strength. Due to a load depending redistribution of the compressive residual stresses this effect is more pronounced for lower loads resulting in the observed change of slope.

The shift of the breakage location of the IND + DR1 variant observed for some specimen is explained by a shift of the weakest specimen location. Those specimens always broke in the transition area (axial to the shaft shown in Figure 2). As described above in this area tensile residual stresses are expected and combined with possible surface defects the observed shift of the breakage location results.

The increase in fatigue strength can be used to reduce the dimensioning of the shafts. To quantify this, the maximum load stresses were first determined for a target fatigue strength of $N = 10^6$ load cycles using the torsional moment at the breakpoint (see Figure 2) and the elastic FE simulation. The geometry of the cross bore was not varied, resulting in no linear relationship between the load stresses and the shaft diameter. A Gaussian process regression model (GPR) was derived on the basis of the FE simulations in order to estimate the load stresses for intermediate

points as well and to reduce the simulation effort. Figure 5 (a) shows the validation of the GPR. For validation, an additional FE simulation was carried out in the area of maximum uncertainty of the GPR. The deviation of the GPR is less than 5 %. In Figure 5 (b) the relationship between the torsional moment, shaft diameter and the maximum Mises stresses is shown. Furthermore, the uncertainty of the GPR is presented.

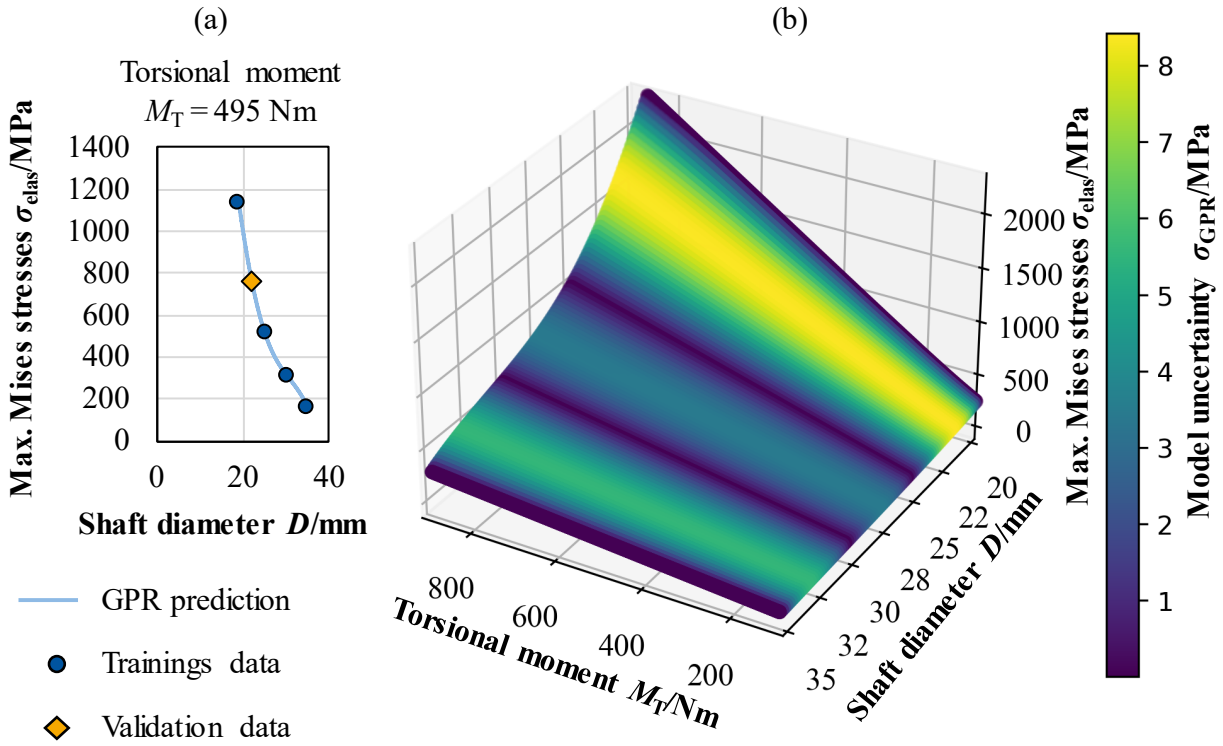

Figure 5: Validation of GPR model (a) and relationship between torsion moment, shaft diameter and maximum Mises stresses as well as the GPR uncertainty (b)

Subsequently, the minimum diameter was determined at which a torsional moment of $T_M = 495.89$ Nm (Torsional moment of REF variant) causes the previously determined maximum load stresses. The results are shown in Table 1. The reduced shaft diameter results in a reduced shaft cross-section and correspondingly reduced specimen weight of 18-37 %.

Table 1: Estimation of the savings potential in terms of the shaft diameter for a target fatigue strength of $N = 10^6$ load cycles

Variant	Torsional moment M_T	Mises stresses for $D = 30$ mm in Mpa	Minimum diameter D_{min} for torsional moment $M_T = 495.89$ Nm in mm
REF	495.89	309.25	30
DR2	647.71	406.33	27.2
DR1	668.81	419.83	26.9
SP2	683.09	428.09	26.7
SP1	694.72	436.39	26.5
IND	722.46	454.13	26.2
IND + DR1	939.32	592.79	23.9

Summary and outlook

In the presented work the cause effect relations between the surface layer properties and the resulting fatigue strength of specimen with cross bores from EN-GJS-700-2 was investigated. The surface layer properties of the cross bore were manipulated using deep rolling, shot peening and induction hardening. The results suggest that the induced tangential compressive residual stresses improve the fatigue strength. Due to a load dependent redistribution of the residual stresses the compressive residual stresses were more effective for lower loads resulting in an improved slope of the S-N curve. Furthermore, the crack initiation location was shifted into the bore due to induction hardening. As a result, the acting load stresses at the crack initiation location was reduced resulting in an increased fatigue strength. The increase in fatigue strength may be used to reduce the dimensions of the shaft resulting in a weight reduction of up to 37 %. In future work, the approach to predict the fatigue strength of the shot peened variant of Reissner et al. will be applied to the induction hardened, the deep rolled and induction hardened and then deep rolled variants [11].

Ackknowledgements

This research was carried out in the framework of the industrial collective research programme (IGF no. 20407 N). It was supported by the Federal Ministry for Economic Affairs and Climate Action (BMWK) through the AiF (German Federation of Industrial Research Associations eV) based on a decision taken by the German Bundestag. Further, the authers would like to thank the ECOROLL AG Werkzeugtechnik for their support in conducting the deep rolling experiments, the Metal Improvement Company LLC for conducting the shot peening experiments, FONDIUM Singen GmbH for manufacturing the specimen cited in this paper and the Institute for Materials Applications in Mechanical Engineering (IWM) of RWTH Aachen University especially Lennart Mirko Scholl and Withold Hildebrandt for the support and provision of the torsion test rig. The authors would also like to thank the Fraunhofer Institute for Structural Durability and System Reliability LBF, in particular Felix Reissner, for the excellent cooperation during the project. Simulations were performed with computing resources granted by RWTH Aachen University under project rwth1215.

References

[1] Federal Climate Change Act: KSG, 2019. [Online]. Available: https://www.gesetze-im-internet.de/englisch_ksg/englisch_ksg.pdf

[2] C. Miki, K. Homma, and T. Tominaga, "High strength and high performance steels and their use in bridge structures," Journal of Constructional Steel Research, vol. 58, no. 1, pp. 3–20, 2002. https://doi.org/10.1016/S0143-974X(01)00028-1

[3] A. Ucharzewski, "Massivumformung - eine Prozesskette für den Leichtbau," (in de), Lightweight Des, vol. 3, no. 2, pp. 42–49, 2010. https://doi.org/10.1007/bf03223603

[4] J. S. Eckersley and B. Ferrelli, "Using Shot Peening to Multiply the Life of Compressor Components," International Compressor Engineering Conference, vol. 1992, Paper 885, 1992.

[5] N. Tsuji, S. Tanaka, and T. Takasugi, "Effect of combined plasma-carburizing and deep-rolling on notch fatigue property of Ti-6Al-4V alloy," Materials Science and Engineering: A, vol. 499, 1-2, pp. 482–488, 2009. https://doi.org/10.1016/j.msea.2008.09.008

[6] U. Kabasakaloglu and H. Saruhan, "Effects of induction hardened surface depth on the dynamic behavior of rotating shaft systems," Materials Testing, vol. 61, no. 3, pp. 277–281, 2019. https://doi.org/10.3139/120.111316

[7] W. Zielecki, M. Bucior, T. Trzepiecinski, and K. Ochał, "Effect of slide burnishing of shoulder fillets on the fatigue strength of X19NiCrMo4 steel shafts," Int J Adv Manuf Technol, vol. 106, 5-6, pp. 2583–2593, 2020. https://doi.org/10.1007/s00170-019-04815-7

[8] S. Woo, Design of mechanical systems: Accelerated lifecycle testing and reliability. Cham: Springer, 2023.

[9] M. O. Görtan and B. Yüksel, "Improvement of Fatigue Properties of EN AW 6082 Aluminum Alloy using Different Deep Rolling Directions," Int. J. Automot. Mech. Eng., vol. 20, no. 2, pp. 10351–10358, 2023. https://doi.org/10.15282/ijame.20.2.2023.02.0800

[10] M. Kobayashi, T. Matsui, and Y. Murakami, "Mechanism of creation of compressive residual stress by shot peening," International Journal of Fatigue, vol. 20, no. 5, pp. 351–357, 1998. https://doi.org/10.1016/S0142-1123(98)00002-4

[11] F. Reissner, L. Uhlmann, J. Baumgartner, T. Herrig, and T. Bergs, "Improved lifetime estimation of shot-peened shaft bores using a numerical approach," Procedia Structural Integrity, 2024.

[12] L. Uhlmann, F. Reissner, S. N. Rathnakar, T. Herrig, J. Baumgartner, and T. Bergs, "Numerical Modeling of the Redistribution of Residual Stresses in Deep Rolled Cross Bores in Shafts from GJS700-2," in Lecture Notes in Mechanical Engineering, Proceedings of the 14th International Conference on the Technology of Plasticity - Current Trends in the Technology of Plasticity: ICTP 2023 - Volume 1, K. Mocellin, P.-O. Bouchard, R. Bigot, and T. Balan, Eds., 1st ed., Cham: Springer Nature Switzerland; Imprint Springer, 2024, pp. 283–290.